

Article

# A Simple Model for the Viscosity of Pickering Emulsions

Rajinder Pal

Department of Chemical Engineering, University of Waterloo, Waterloo, ON N2L 3G1, Canada; rpal@uwaterloo.ca; Tel.: +1-519-888-4567 (ext. 32985)

Received: 23 November 2017; Accepted: 22 December 2017; Published: 23 December 2017

**Abstract:** A new model is proposed for the viscosity of Pickering emulsions at low shear rates. The model takes into consideration the increase in the effective volume fraction of droplets, due to the presence of an interfacial layer of solid nanoparticles at the oil-water interface. The model also considers aggregation of droplets and eventual jamming of Pickering emulsion at high volume fraction of dispersed phase. According to the proposed model, the relative viscosity of a Pickering emulsion at low shear rates is dependent on three factors: contact angle, ratio of bare droplet radius to solid nanoparticle radius, and the volume fraction of bare droplets. For a given radius of nanoparticles, the relative viscosity of a Pickering emulsion increases with the decrease in bare droplet radius. For O/W Pickering emulsions, the relative viscosity decreases with the increase in contact angle. The W/O Pickering emulsion exhibits an opposite behavior in that the relative viscosity increases with the increase in contact angle. The proposed model describes the experimental viscosity data for Pickering emulsions reasonably well.

**Keywords:** Pickering emulsions; contact angle; nanoparticles; interface; rheology; viscosity

## 1. Introduction

Pickering emulsions, also referred to as Ramsden emulsions, are dispersions of two immiscible liquids (oil and water) where the dispersed droplets are stabilized against coalescence solely by the presence of solid particles, usually nanoparticles, at the oil-water interface. Figure 1 shows a schematic diagram of a droplet of Pickering emulsion. The droplet has a “core-shell” morphology, where the “core” is composed of liquid phase and the “shell” consists of an interfacial layer of solid nanoparticles.

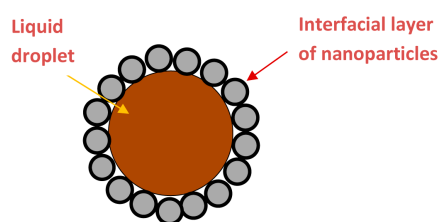


Figure 1. Droplet of a Pickering emulsion.

There has been a rapid growth of interest in nanoparticles-stabilized Pickering emulsions in recent years due to their many potential applications in industries such as: food, pharmaceutical, petroleum, biomedical, environment, cosmetics, and catalysis [1–18]. A recent article by Binks [16] discusses many potential applications of Pickering emulsions. The biomedical and pharmaceutical applications are discussed at length in a paper by Wu and Ma [1]. In a series of articles by Leclercq and Nardello-Rataj group [19–22], the applications of Pickering emulsions in interfacial catalysis for biphasic systems are

discussed. For example, reactions can be carried out simultaneously in both aqueous and non-aqueous phases by placing solid catalyst nanoparticles at the oil-water interface [18–22]. The solid nanoparticles placed at the oil-water interface serve the dual purpose of catalyst and emulsion stabilizer.

For solid particles to be adsorbed at the oil-water interface, it is necessary that the particles are partially wetted by both oil and water phases. When solid particles adsorb at the oil-water interface, they reduce the interfacial area of the high energy oil-water interface. Thus, the driving force for the transfer of particles at the interface is the reduction of the interfacial area. Depending on the relative wettability of the liquid phases for the solid nanoparticles, two types of emulsions could be formed: oil-in-water (O/W) emulsion, where oil forms the droplets and water is the continuous phase, and water-in-oil (W/O) emulsion, where water forms the droplets and oil is the continuous phase. The liquid phase, which preferentially wets the solid particles tends to become the continuous phase of the emulsion and the liquid phase, which is relatively less wetting of the solid particles becomes the dispersed phase. The relative wettability of the liquid phases for the solid particles is determined by the three-phase contact angle  $\theta$ . If the contact angle measured through the aqueous phase, as shown in Figure 2, is greater than  $90^\circ$ , then the solid particles are relatively more wetted by the oil phase, and in such situations, W/O emulsions are generally formed. When the contact angle  $\theta$  is less than  $90^\circ$ , the solid particles are preferentially wetted by the aqueous phase and in such situations, O/W emulsions are favored. When  $\theta = 90^\circ$ , both liquid phases wet the solid particles equally, and in such situations, there is no preferred emulsion—O/W or W/O.

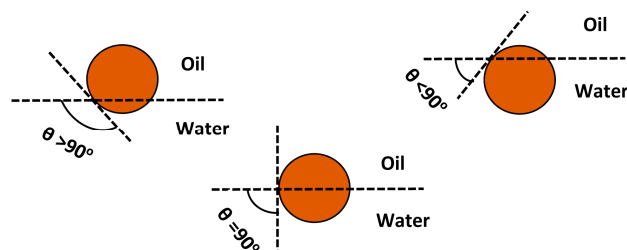


Figure 2. Different wetting conditions described in terms of contact angle  $\theta$ .

The energy required to desorb a single solid nanoparticle from the oil-water interface is given as [8]:

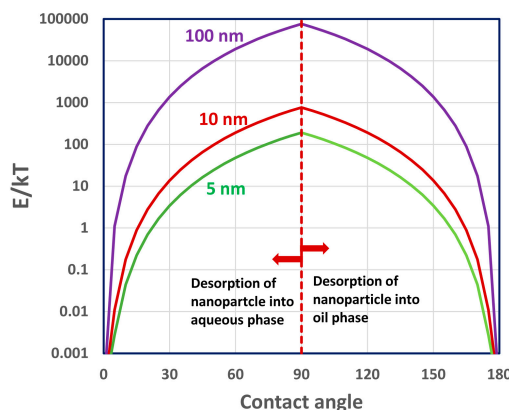
$$E = \pi R_{np}^2 \gamma_{OW} (1 \pm \cos \theta)^2 \tag{1}$$

where  $E$  is the energy required to desorb a single solid nanoparticle of radius  $R_{np}$  from the oil-water interface with interfacial tension  $\gamma_{OW}$ . The plus sign in the brackets gives the energy that is required for desorption of a nanoparticle from oil-water interface into the oil phase, and the negative sign gives energy for desorption of a nanoparticle into the aqueous phase. Equation (1) could be re-written in dimensionless form as:

$$E/kT = \pi R_{np}^2 \gamma_{OW} (1 \pm \cos \theta)^2 / kT \tag{2}$$

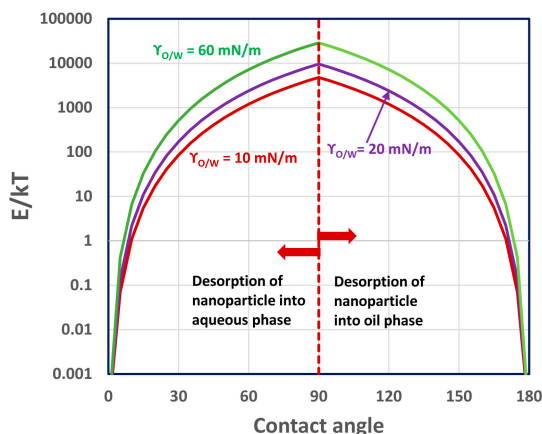
where  $k$  is the Boltzmann constant and  $T$  is the absolute temperature. This Equation (2) gives the desorption energy relative to thermal energy of a particle.

Figure 3 shows the plots of relative desorption energy of a nanoparticle from the oil-water interface as a function of contact angle. The plots are shown for different values of nanoparticle radius (ranging from 5 nm to 100 nm). The interfacial tension  $\gamma_{OW}$  is fixed at 10 mN/m. The relative desorption energy needed to desorb a nanoparticle from the oil-water interface to the aqueous phase decreases with the decrease in contact angle. The relative desorption energy needed to desorb a nanoparticle from the oil-water interface to the oil phase decreases with the increase in contact angle.



**Figure 3.** Relative desorption energy of a single solid nanoparticle as a function of contact angle  $\theta$  for different values of nanoparticle radius.

The desorption energy of a nanoparticle also depends on the interfacial tension  $\gamma_{OW}$ . Figure 4 shows the plots of relative desorption energy for different values of interfacial tension. The radius of the nanoparticle is fixed at 25 nm. As the interfacial tension increases, the relative desorption energy increases. The effect of interfacial tension on the desorption energy is less severe in comparison with the effect of nanoparticle size, as expected from Equation (2).



**Figure 4.** Relative desorption energy of a single solid nanoparticle as a function of contact angle  $\theta$  for different values of interfacial tension.

The desorption energy should be significantly larger than the thermal energy in order to produce a stable emulsion. In general, the contact angle for the stabilization of O/W emulsions should be in the range  $15^\circ < \theta < 90^\circ$  [23]. For stable W/O emulsions to be produced, the contact angle should be in the range  $90^\circ < \theta < 165^\circ$  [23]. If the solid nanoparticles are too hydrophobic,  $\theta \approx 180^\circ$ , then the nanoparticles remain dispersed in the oil phase, and consequently, the W/O emulsions produced are unstable. Similarly, if the nanoparticles are too hydrophilic, that is,  $\theta \approx 0^\circ$ , they remain dispersed in the aqueous phase, and hence fail to produce stable O/W emulsions.

## 2. Rheology of Emulsions without any Interfacial Additives

The rheological constitutive equation for a dilute emulsion of identical droplets can be developed based on a single-droplet mechanics [24,25]. The development of the constitutive equation requires knowledge of the velocity, pressure, and stress fields around a single droplet, and the evolution of the shape of a single droplet, when the droplet is subjected to a shear flow. The flow fields in

and around the droplet are calculated using the Navier-Stokes equations subject to the appropriate boundary conditions, such as: (i) continuity of tangential and normal velocities at the oil-water interface; (ii) continuity of tangential stresses at the interface; and, (iii) discontinuity of normal stress across the interface. Under the conditions of zero-order (infinitesimal) deformation of droplets (small capillary number) and the absence of any interfacial additives (surfactant or nanoparticles), the rheological constitutive equation for a dilute emulsion of two immiscible Newtonian liquids is given as:

$$\bar{\sigma} = -P\bar{\delta} + 2\eta_c \left( 1 + \frac{2 + 5\lambda}{2 + 2\lambda} \varphi \right) \bar{E} \tag{3}$$

where  $\bar{\sigma}$  is the bulk stress tensor,  $P$  is the average pressure,  $\bar{\delta}$  is the unit tensor,  $\bar{E}$  is the bulk rate of strain tensor,  $\eta_c$  is the viscosity of the continuous phase,  $\lambda$  is the ratio of dispersed-phase viscosity to continuous-phase viscosity, and  $\varphi$  is the volume fraction of the dispersed phase. From Equation (3), it follows that the effective viscosity of a dilute emulsion is:

$$\eta = \eta_c \left[ 1 + \frac{2 + 5\lambda}{2 + 2\lambda} \varphi \right] \tag{4}$$

Equation (4) is referred to as the Taylor emulsion viscosity equation [26]. It could also be expressed as:

$$\eta_r = \eta / \eta_c = \left[ 1 + \frac{2 + 5\lambda}{2 + 2\lambda} \varphi \right] \tag{5}$$

where  $\eta_r$  is the relative viscosity defined as the ratio of emulsion viscosity to continuous phase viscosity. From Equation (5), the intrinsic viscosity  $[\eta]$  of an emulsion is as follows:

$$[\eta] = \lim_{\varphi \rightarrow 0} \left( \frac{\eta_r - 1}{\varphi} \right) = \left( \frac{2 + 5\lambda}{2 + 2\lambda} \right) \tag{6}$$

For dilute suspensions of rigid hard spheres, Equation (5) reduces to the well-known Einstein suspension viscosity equation [27,28]:

$$\eta_r = \eta / \eta_c = [1 + 2.5\varphi] \tag{7}$$

Note that the intrinsic viscosity of suspension of hard spheres has a constant value of 2.5 whereas the intrinsic viscosity of emulsion is dependent on the viscosity ratio  $\lambda$  (see Equation (6)).

The Einstein suspension viscosity equation as well as the Taylor emulsion viscosity equation are valid only for very dilute systems. Several authors [29–33] have developed viscosity equations for non-dilute dispersed systems taking into account the packing limits of particles and droplets. The following equation proposed by Krieger and Dougherty [31] is quite popular in the literature available on the viscosity equations for concentrated suspensions of rigid particles:

$$\eta_r = \left( 1 - \frac{\varphi}{\varphi_m} \right)^{-2.5\varphi_m} \tag{8}$$

where  $\varphi_m$  is the maximum packing volume fraction of particles where the relative viscosity of suspension diverges.

Pal [30] has extended the Taylor emulsion viscosity equation for dilute systems to concentrated emulsions using the differential effective medium approach and taking into consideration the packing limits of droplets. He proposed the following equation for the viscosity of concentrated emulsions at low shear rates:

$$\eta_r \left[ \frac{2\eta_r + 5\lambda}{2 + 5\lambda} \right]^{3/2} = \left( 1 - \frac{\varphi}{\varphi_m} \right)^{-2.5\varphi_m} \tag{9}$$

In the limit  $\lambda \rightarrow \infty$  (rigid particles), Equation (9) reduces to the Krieger-Dougherty Equation (8). In the limit  $\varphi \rightarrow 0$ , Equation (9) reduces to the Taylor emulsion viscosity equation for dilute emulsions. This equation is found to adequately describe a large pool of available viscosity data on unstable (without interfacial additives) and surfactant-stabilized emulsions.

### 3. Rheology of Pickering Emulsions—Brief Literature Review

As noted in the preceding section, the rheology of traditional emulsions (surfactant-stabilized emulsions and emulsions without any interfacial additives) is well understood. Models are available to predict a priori the rheological properties of such emulsions. However, the rheology of Pickering emulsions stabilized by solid amphiphilic nanoparticles has received a limited attention.

Binks et al. [34] experimentally studied the rheological behavior of W/O emulsions stabilized by hydrophobic bentonite clay particles. The emulsions exhibited shear-thinning and yield stresses due to the formation of a network structure of clay particles and water droplets. Wolf et al. [35] investigated the rheology of Pickering O/W emulsions stabilized by hydrophilic silica nanoparticles. The droplets were coated by a monolayer of closely packed silica nanoparticles. At high volume fractions of oil droplets, the emulsions exhibited shear-thickening behavior at intermediate shear rates. The shear-thickening behavior is frequently observed in suspensions of rigid particles, but not in traditional emulsions. Thus, the authors concluded that the droplets of oil coated with monolayers of solid nanoparticles behave more like rigid spheres. Katepalli et al. [36] investigated the effects of nanoparticles shape and inter-particle interactions on the rheology of Pickering O/W emulsions at a fixed volume fraction of oil of 0.50. The spherical silica nanoparticles stabilized the emulsion by forming a hexagonally packed monolayer of particles at the oil-water interface. The non-spherical fumed silica nanoparticles stabilized emulsion droplets by forming an interlocked network of particles at the oil-water interface. At high salt concentrations, the interparticle interactions were attractive, resulting in a network of nanoparticles and emulsion droplets, and consequently, non-Newtonian rheology. Braisch et al. [37] studied the viscosity behavior of O/W emulsions stabilized by hydrophilic silica nanoparticles. However, the matrix of emulsions was thickened by a polymer (polyethylene glycol, PEG 6000). The droplets were fully covered by a monolayer of silica nanoparticles. The O/W Pickering emulsions thickened by PEG exhibited shear-thinning behavior. Ganley and Van duijnveldt [38] investigated the rheology of O/W Pickering emulsions that were stabilized by montmorillonite clay platelets. The clay was present in excess of what was needed to fully coat the oil droplets. The excess clay platelets formed a network structure in the matrix phase imparting non-Newtonian rheology to emulsions. Hermes and Clegg [39] studied the rheology, including yielding behavior, of highly concentrated O/W emulsions (also referred to as emulsion gels) stabilized by silica nanoparticles. The Pickering O/W emulsion gels were viscoelastic in nature and exhibited yield stress.

In summary, the rheology of Pickering emulsions stabilized by solid nanoparticles is not as well understood as that of traditional surfactant-stabilized emulsions. Little or no work has been reported on modelling of the rheological behavior of Pickering emulsions. The experimental studies that are reported in the literature on the rheology of Pickering emulsions often deal with complicated systems where the non-Newtonian behavior is caused by factors, such as: network formation of droplets and nanoparticles; network of films of matrix phase in highly concentrated emulsion gels; and incorporation of thickeners (clays, polymers) in the matrix phase.

## 4. Modelling of the Viscosity of Pickering Emulsions

### 4.1. Dilute Pickering Emulsions

Consider a single “core-shell” droplet of a Pickering emulsion, as shown in Figure 1. While the core of the composite droplet is mobile, the presence of a rigid interfacial layer of solid nanoparticles at the surface of the droplet disrupts the transmission of tangential and normal stresses from the

continuous phase liquid to the core liquid. Thus, the composite “core-shell” droplets of a Pickering emulsion can be treated as rigid particles of effective radius  $R_{eff}$  given as:

$$R_{eff} = R_d + h \tag{10}$$

where  $R_d$  is the radius of the core droplet and  $h$  is the thickness of the solid nanoparticle layer protruding into the continuous phase (see Figure 5).

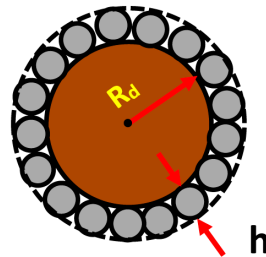


**Figure 5.** Composite “core-shell” droplet of a Pickering emulsion with core radius  $R_d$  and interfacial layer thickness  $h$  protruding into the continuous phase.

It should be noted that the thickness of the rigid interfacial layer  $h$  protruding into the continuous phase is governed by the contact angle  $\theta$  and radius of interfacial nanoparticles  $R_{np}$ . Consider a single solid nanoparticle present at the oil-water interface, as shown in Figure 6. The solid nanoparticle is assumed to be present at the interface of an oil droplet. From the figure, it is clear that the thickness of the interfacial layer protruding into the continuous phase (aqueous phase in Figure 6) can be expressed in terms of the contact angle  $\theta$  and radius of interfacial nanoparticles  $R_{np}$  as follows:

$$h = R_{np}(1 + \cos \theta) \tag{11}$$

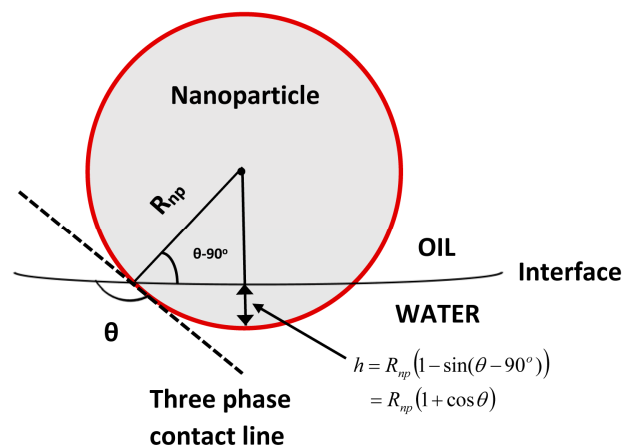


**Figure 6.** Determination of interfacial thickness of solid nanoparticles protruding into the continuous phase of an emulsion.

Equation(11) is valid for O/W emulsions. For W/O emulsions, the thickness of the interfacial layer protruding into the continuous phase is:

$$h = R_{np}(1 - \cos \theta) \tag{12}$$

The increase in the effective volume fraction of droplets due to the presence of an interfacial monolayer of solid nanoparticles at the oil-water interface can be expressed in terms of the layer thickness as:

$$\varphi_S = \varphi \left( 1 + \frac{h}{R_d} \right)^3 \tag{13}$$

where  $\varphi_S$  is the effective volume fraction of composite core-shell droplets and  $\varphi$  is the volume fraction of bare droplets without interfacial layer of solid nanoparticles.

As composite droplets are assumed to behave as rigid particles, the relative viscosity of dilute Pickering emulsions can be calculated from the Einstein viscosity equation:

$$\eta_r = \eta/\eta_c = [1 + 2.5\varphi_S] \tag{14}$$

where  $\varphi_S$  is given by Equation (13).

#### 4.2. Concentrated Pickering Emulsions

The modified Einstein equation, Equation (14), is valid only in the limit  $\varphi_S \rightarrow 0$ . We can re-write Equation (5) as:

$$\eta_r = 1 + 2.5 \left( \frac{\text{Volume of composite droplets}}{\text{Total volume of emulsion}} \right) \tag{15}$$

Pal [40] has argued that it is the free volume available to the inclusions that is more relevant in determining the viscosity of non-dilute dispersed systems. Accordingly, the following equation is applicable to concentrated Pickering emulsions:

$$\eta_r = 1 + 2.5 \left( \frac{\text{Volume of composite droplets}}{\text{Free volume available to emulsion}} \right) \tag{16}$$

From Equation (16), it follows that:

$$\eta_r = 1 + 2.5 \left( \frac{\varphi_S}{1 - \varphi_S} \right) \tag{17}$$

This equation is applicable at low to moderate volume fractions of composite droplets. At high concentrations of dispersed phase, clustering of droplets dominates. When clusters are formed, a significant amount of continuous-phase fluid is trapped within the clusters resulting in an increase in the effective dispersed phase concentration. At glass transition concentration of composite droplets  $\varphi_g$ , the entire emulsion is jammed into a single large cluster. In the jammed or arrested state of the emulsion, the emulsion is expected to behave as a semi-solid with significant yield-stress. Figure 7 schematically shows the change in emulsion morphology, with the increase in volume fraction of composite droplets.

In order to take into account the aggregation of droplets in Pickering emulsions, Equation (17) is modified as follows:

$$\eta_r = 1 + 2.5 \left( \frac{\varphi_{eff}}{1 - \varphi_{eff}} \right) \tag{18}$$

where  $\varphi_{eff}$  is the effective volume fraction of the dispersed phase. The relationship between  $\varphi_{eff}$  and  $\varphi_S$  can be developed on the following basis: (a) in the dilute limit  $\varphi_S \rightarrow 0$ ,  $\varphi_{eff} = \varphi_S$ ; (b) in the jammed state limit  $\varphi_S \rightarrow \varphi_g$ ,  $\varphi_{eff} = 1$ ; (c)  $\partial(\varphi_{eff}/\varphi_S)/\partial\varphi_S \geq 0$ ; and (d) in the limit  $\varphi_S \rightarrow \varphi_g$ ,  $\partial(\varphi_{eff}/\varphi_S)/\partial\varphi_S = 0$ .

The following empirical expression meets all of the conditions just mentioned, and has been found to describe aggregation behavior of a variety of dispersed systems [40–42]:

$$\varphi_{eff}/\varphi_S = \left[ 1 + \left( \frac{1 - \varphi_g}{\varphi_g} \right) \left( \sqrt{1 - \left( \frac{\varphi_g - \varphi_S}{\varphi_g} \right)^2} \right) \right] \quad (19)$$

In summary, the model proposed in this work for the viscosity of dilute to concentrated Pickering emulsions at low shear rates is Equation (18) in conjunction with Equations (11)–(13) and (19).

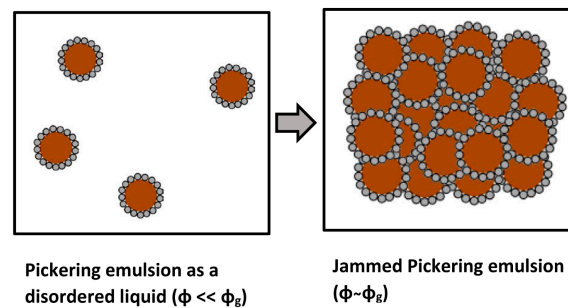


**Figure 7.** Change in morphology of Pickering emulsion with the increase in composite droplets concentration.

#### 4.3. Limitations of the Proposed Model

The proposed model has the following restrictions: the solid nanoparticles are spherical in shape; the solid nanoparticles coat the surface of the emulsion droplets by forming a monolayer of closely packed nanoparticles; the excess nanoparticles, over and above the amount that is needed to form a closely packed monolayer on the surface of the emulsion droplets, simply enhance the viscosity of the matrix phase without any network structure formation; the nanoparticles-coated droplets behave as rigid hard spheres; and, the composite nanoparticles-coated droplets are reasonably monodisperse. Some of these assumptions such as hard-sphere interactions and mono-dispersity of droplets can be relaxed if the glass-transition concentration  $\varphi_g$  is taken to be an adjustable parameter. The jamming concentration of emulsion droplets is clearly dependent on the type of interactions and the size distribution of emulsion droplets.

### 5. Predictions of the Proposed Viscosity Model for Pickering Emulsions

According to the proposed model, the relative viscosity of a Pickering emulsion (O/W or W/O) is a function of the following factors: (a) volume fraction of bare droplets (without interfacial nanoparticle layers); (b) the relative size of nanoparticles to bare droplets; and, (c) contact angle. Figure 8 shows the model predictions for the relative viscosity O/W Pickering emulsion as a function of volume fraction of bare droplets for different values of  $R_d/R_{np}$ , ranging from 10 to 40. The contact angle is taken to be  $45^\circ$  and the glass transition volume fraction of composite droplets where jamming of Pickering emulsion is expected is taken as 0.58. Clearly, the relative viscosity is strongly dependent on the relative sizes of the nanoparticles and bare droplets. For a given bare droplet radius, the relative viscosity increases with the increase in the radius of the nanoparticles at any given volume fraction of bare droplets. The effect of contact angle  $\theta$  on the relative viscosity of O/W and W/O emulsions, as predicted by the model, is shown in Figure 9. The  $R_d/R_{np}$  ratio is fixed at 10 and the glass transition volume fraction of composite droplets is 0.58. For O/W emulsions, the relative viscosity at any given volume fraction of bare droplets decreases with the increase in contact angle. A reverse behavior is observed in the case of W/O emulsions where the relative viscosity increases with the increase in contact angle.

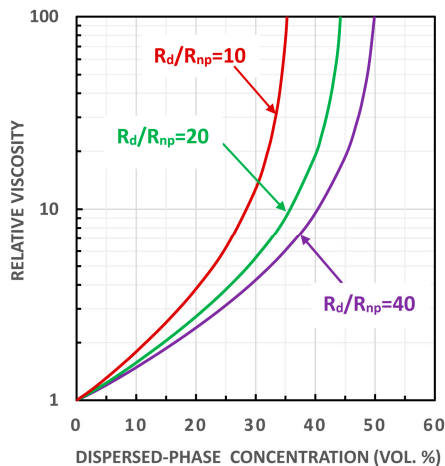


**Figure 8.** Model predictions of relative viscosity versus dispersed-phase (bare droplets) concentration (vol. %) of oil-in-water (O/W) Pickering emulsions for different ratios of bare droplet radius to nanoparticle radius.

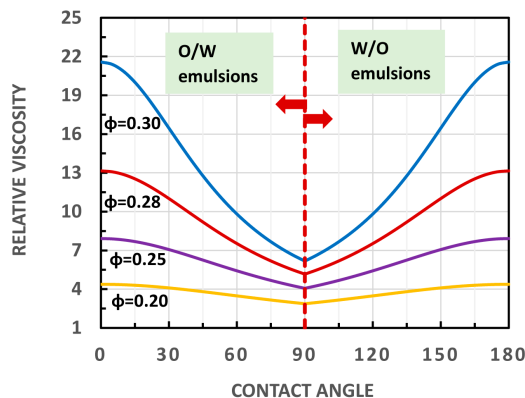
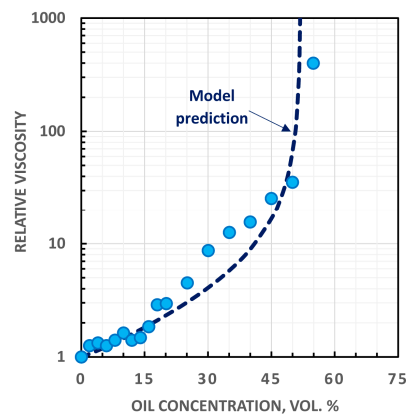


**Figure 9.** Model predictions of relative viscosity versus contact angle of oil-in-water (O/W) and water-in-oil (W/O) Pickering emulsions for different volume fractions of bare droplets.

### 6. Comparison of Model Predictions with Experimental Data

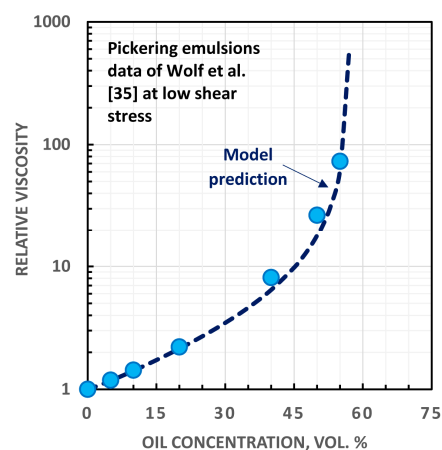
The experimental viscosity data for Pickering O/W emulsions were collected using a co-axial cylinder viscometer. The emulsions were prepared using hydrophilic starch nanoparticles at 2 wt % concentration in the aqueous phase. The oil used was a white mineral oil, which was supplied by Petro-Canada. The oil viscosity was 21 mPa s at 28 °C. The average diameter of the nanoparticles was 20.9 nm and the average droplet diameter was 91.7 μm. The contact angle was 46°, as reported in our earlier study [43]. The viscosity measurements were carried out at a temperature of about 28 °C.

Figure 10 compares the low shear relative viscosity data of Pickering O/W emulsions stabilized by starch nanoparticles with the proposed model. The experimental relative viscosity data for Pickering O/W emulsions can be described reasonably well by the model using the glass transition volume fraction of 0.52. This volume fraction of droplets where viscosity divergence occurs is lower than the reported literature value of 0.58 corresponding to glass transition concentration of mono-sized hard spheres. This is not unexpected, given that the emulsions are not monodisperse. Furthermore, due to the large size of the droplets, the droplets also probably undergo some deformation when they are subjected to a shear field.



**Figure 10.** Comparison of the experimental relative viscosity data for Pickering O/W emulsions with the predictions of the proposed model.

Figure 11 compares the experimental low-shear viscosity data of Wolf et al. [35] with the proposed model. The experimental data were obtained for O/W emulsions that were stabilized by hydrophilic silica nanoparticles. The Sauter mean diameter of emulsion droplets was  $3.15 \mu\text{m}$ . The silica nanoparticles had an average diameter of  $8 \text{ nm}$ . Although the contact angle was not reported, it is assumed to be  $45^\circ$ . Due to small sized nanoparticles relative to the droplet size (large  $R_d/R_{np}$  ratio of approximately 394), the predictions of the proposed model are insensitive to contact angle. Interestingly, the model prediction using the glass transition concentration of monodisperse hard spheres of 0.58 is in excellent agreement with the experimental viscosity data of Wolf et al. [35], as obtained for Pickering O/W emulsions at a low shear stress of  $0.2 \text{ Pa}$ . Note that the Pickering emulsions that were prepared by Wolf et al. consisted of relatively much smaller droplets as compared with the emulsions of Figure 10. The droplets of Figure 10 emulsions were nearly 30 times larger than the droplets of emulsions prepared by Wolf et al. Thus, the Pickering emulsions prepared by Wolf et al. are closer to the assumptions made in the proposed model.



**Figure 11.** Comparison of the literature relative viscosity data for Pickering O/W emulsions with the predictions of the proposed model.

## 7. Conclusions

The viscosity behavior of nanoparticles-stabilized Pickering emulsions is studied. A new model is developed to describe and to predict the viscosity of Pickering emulsion as a function of volume fraction of bare droplets. The droplets of Pickering emulsion are modelled as “core-shell” droplets with liquid core and interfacial layer of solid nanoparticles as shell. As the presence of an interfacial rigid

layer of solid nanoparticles at the oil-water interface disrupts the transmission of tangential and normal stresses from the continuous phase to the inner core liquid, the composite “core-shell” droplets behave as rigid particles of effective radius larger than the radius of bare droplets. The effective radius of composite droplets is dependent on the contact angle and the size of the interfacial solid nanoparticles. The viscosity model that is proposed in this study takes into consideration of clustering of composite droplets and eventual jamming of Pickering emulsion at high volume fraction of dispersed droplets. For a given size nanoparticles, the viscosity of Pickering emulsion increases with the decrease in bare droplet size. The contact angle also has a significant effect on the viscosity of Pickering emulsion. For O/W type Pickering emulsion, the viscosity decreases with the increase in contact angle, whereas the W/O type Pickering emulsion exhibits an opposite behavior, that is, the viscosity increases with the increase in contact angle. The proposed model describes the experimental viscosity data for Pickering emulsions reasonably well. More experimental work is needed on the low-shear viscosity behavior of well-characterized Pickering emulsions to validate the proposed model.

**Acknowledgments:** Financial support from the Natural Sciences and Engineering Research Council of Canada (NSERC) is appreciated. Upinder Bains assisted in the measurement of the viscosity of starch-stabilized emulsions.

**Conflicts of Interest:** The author declares no conflict of interest.

## References

1. Wu, J.; Ma, G.H. Recent studies of Pickering emulsions: Particles make the difference. *Small* **2006**, *12*, 4633–4648. [[CrossRef](#)] [[PubMed](#)]
2. Yang, Y.; Fang, Z.; Chen, X.; Zhang, W.; Xie, Y.; Chen, Y.; Liu, Z.; Yuan, W. An overview of Pickering emulsions: Solid-particle materials, classification, morphology, and applications. *Front. Pharmacol.* **2017**, *3*, 287. [[CrossRef](#)] [[PubMed](#)]
3. Berton-Carabin, C.C.; Schroen, K. Pickering emulsions for food applications: Background, trends, and challenges. *Annu. Rev. Food Sci. Technol.* **2015**, *6*, 263–297. [[CrossRef](#)] [[PubMed](#)]
4. Chevalier, Y.; Bolzinger, M.A. Emulsions stabilized with solid nanoparticles: Pickering emulsions. *Colloids Surf. A* **2013**, *439*, 23–34. [[CrossRef](#)]
5. Timgren, A.; Rayner, M.; Dejmek, P.; Marku, D.; Sjo, M. Emulsion stabilizing capacity of intact starch granules modified by heat treatment or octenyl succinic anhydride. *Food Sci. Nutr.* **2013**, *1*, 157–171. [[CrossRef](#)] [[PubMed](#)]
6. Zoppe, J.O.; Venditti, R.A.; Rojas, O.J. Pickering emulsions stabilized by cellulose nanocrystals grafted with thermos-responsive polymer brushes. *J. Colloid Interface Sci.* **2012**, *369*, 202–209. [[CrossRef](#)] [[PubMed](#)]
7. Chen, X.; Song, X.; Huang, J.; Wu, C.; Ma, D.; Tian, M.; Jiang, H.; Huang, P. Phase behavior of Pickering emulsions stabilized by graphene oxide sheets and resins. *Energy Fuels* **2017**, *31*, 13439–13447. [[CrossRef](#)]
8. Binks, B.P.; Fletcher, P.D.I.; Holt, B.L.; Beaussoubre, P. Phase inversion of particle-stabilized perfume oil-water emulsions: Experiment and theory. *Phys. Chem. Chem. Phys.* **2010**, *12*, 11954–11966. [[CrossRef](#)] [[PubMed](#)]
9. Fournier, C.O.; Fradette, L.; Tanguy, P.A. Effect of dispersed phase viscosity on solid-stabilized emulsions. *Chem. Eng. Res. Des.* **2009**, *87*, 499–506. [[CrossRef](#)]
10. Tsabet, E.; Fradette, L. Effect of the properties of oil, particles, and water on the production of Pickering emulsions. *Chem. Eng. Res. Des.* **2015**, *97*, 9–17. [[CrossRef](#)]
11. Simon, S.; Theiler, S.; Knudsen, A.; Oye, G.; Sjoblom, J. Rheological properties of particle-stabilized emulsions. *J. Dispers. Sci. Tech.* **2010**, *31*, 632–640. [[CrossRef](#)]
12. Li, C.; Liu, Q.; Mei, Z.; Wang, J.; Xu, J.; Sun, D. Pickering emulsions stabilized by paraffin wax and laponite clay particles. *J. Colloid Interface Sci.* **2009**, *336*, 314–321. [[CrossRef](#)] [[PubMed](#)]
13. Tarimala, S.; Wu, C.Y.; Dai, L.L. Pickering emulsions—A paradigm shift. In Proceedings of the 05AICHE: 2005 AICHE Annual Meeting and Fall Showcase, Cincinnati, OH, USA, 30 October–4 November 2005.
14. Dickinson, E. Use of nanoparticles and microparticles in the formation and stabilization of food emulsions. *Trends Food Sci. Technol.* **2012**, *24*, 4–12. [[CrossRef](#)]
15. Dickinson, E. Food emulsions and foams: Stabilization by particles. *Curr. Opin. Colloid Interface Sci.* **2010**, *15*, 40–49. [[CrossRef](#)]

16. Binks, B.P. Colloidal particles at a range of fluid-fluid interfaces. *Langmuir* **2017**, *33*, 6947–6963. [[CrossRef](#)] [[PubMed](#)]
17. Leclercq, L.; Nardello-Rataj, V. Pickering emulsions based on cyclodextrin: A smart solution for antifungal azole derivatives topical delivery. *Eur. J. Pharm. Sci.* **2016**, *82*, 126–137. [[CrossRef](#)] [[PubMed](#)]
18. Crossley, S.; Faria, J.; Shen, M.; Resasco, D.E. Solid nanoparticles that catalyze biofuel upgrade reactions at the water/oil interface. *Science* **2010**, *327*, 68–72. [[CrossRef](#)] [[PubMed](#)]
19. Yang, B.; Leclercq, L.; Clacens, J.M.; Nardello-Rataj, V. Acidic/amphiphilic silica nanoparticles: New eco-friendly Pickering interfacial catalysis for biodiesel production. *Green Chem.* **2017**, *19*, 4552–4562. [[CrossRef](#)]
20. Pera-Titus, M.; Leclercq, L.; Clacens, J.M.; De Campo, F.; Nardello-Rataj, V. Pickering interfacial catalysis for biphasic systems: From emulsion design to green reactions. *Angew. Chem. Int. Ed.* **2015**, *54*, 2006–2021. [[CrossRef](#)] [[PubMed](#)]
21. Leclercq, L.; Company, R.; Muhlbauer, A.; Mouret, A.; Aubry, J.M.; Nardello-Rataj, V. Versatile eco-friendly Pickering emulsions based on substrate/native cyclodextrin complexes: A winning approach for solvent-free oxidations. *ChemSusChem* **2013**, *6*, 1533–1540. [[CrossRef](#)] [[PubMed](#)]
22. Leclercq, L.; Mouret, A.; Proust, A.; Schmitt, V.; Bauduin, P.; Aubry, J.M.; Nardello-Rataj, V. Pickering emulsions stabilized by catalytic polyoxometalate nanoparticles: A new effective medium for oxidation reactions. *Chem. Eur. J.* **2012**, *18*, 14352–14358. [[CrossRef](#)] [[PubMed](#)]
23. Kaptay, G. On the equation of the maximum capillary pressure induced by solid particles to stabilize emulsions and foams and on the emulsion stability diagrams. *Colloids Surf. A* **2006**, *282/283*, 387–401. [[CrossRef](#)]
24. Pal, R. *Rheology of Particulate Dispersions and Composites*; CRC P: Boca Raton, FL, USA, 2007.
25. Pal, R. Fundamental rheology of disperse systems based on single-particle mechanics. *Fluids* **2016**, *1*, 40. [[CrossRef](#)]
26. Taylor, G.I. The viscosity of a fluid containing small drops of another liquid. *Proc. R. Soc. Lond. A* **1932**, *138*, 41–48. [[CrossRef](#)]
27. Einstein, A. Eine neue Bestimmung der Molekuldimension. *Ann. Phys.* **1906**, *19*, 289–306. [[CrossRef](#)]
28. Einstein, A. Berichtigung zu meiner Arbeit: Eine neue Bestimmung der Molekuldimension. *Ann. Phys.* **1911**, *34*, 591–592. [[CrossRef](#)]
29. Pal, R. Single parameter and two parameter rheological equations of state for nondilute emulsions. *Ind. Eng. Chem. Res.* **2001**, *40*, 5666–5674. [[CrossRef](#)]
30. Pal, R. Novel viscosity equations for emulsions of two immiscible liquids. *J. Rheol.* **2001**, *45*, 509–520. [[CrossRef](#)]
31. Krieger, I.M.; Dougherty, T.J. Mechanism for non-Newtonian flow in suspensions of rigid particles. *Trans. Soc. Rheol.* **1959**, *3*, 137–152. [[CrossRef](#)]
32. Mooney, M. The viscosity of a concentrated suspension of spherical particles. *J. Colloid Sci.* **1951**, *6*, 162–170. [[CrossRef](#)]
33. Pal, R.; Yan, Y.; Masliyah, J. Rheology of emulsions. In *Emulsions: Fundamentals and Applications in the Petroleum Industry*. *Adv. Chem. Ser.* **1992**, *231*, 131–170.
34. Binks, B.P.; Clint, J.H.; Whitby, C.P. Rheological behavior of water-in-oil emulsions stabilized by hydrophobic bentonite particles. *Langmuir* **2005**, *21*, 5307–5316. [[CrossRef](#)] [[PubMed](#)]
35. Wolf, B.; Lam, S.; Kirkland, M.; Frith, W.J. Shear-thickening of an emulsion stabilized with hydrophilic silica particles. *J. Rheol.* **2007**, *51*, 465–478. [[CrossRef](#)]
36. Katepalli, H.; John, V.T.; Tripathi, A.; Bose, A. Microstructure and rheology of particle stabilized emulsions: Effects of particle shape and inter-particle interactions. *J. Colloid Interface Sci.* **2017**, *485*, 11–17. [[CrossRef](#)] [[PubMed](#)]
37. Braisch, B.; Kohler, K.; Schuchmann, H.P.; Wolf, B. Preparation and flow behavior of oil-in-water emulsions stabilized by hydrophilic silica particles. *Chem. Eng. Technol.* **2009**, *32*, 1107–1112. [[CrossRef](#)]
38. Ganley, W.J.; Van Duijneveldt, J.S. Controlling the rheology of montmorillonite stabilized oil-in-water emulsions. *Langmuir* **2017**, *33*, 1679–1686. [[CrossRef](#)] [[PubMed](#)]
39. Hermes, M.; Clegg, P.S. Yielding and flow of concentrated Pickering emulsions. *Soft Matter* **2013**, *9*, 7568–7575. [[CrossRef](#)]

40. Pal, R. Viscosity-concentration relationships for nanodispersions based on glass transition point. *Can. J. Chem. Eng.* **2017**, *95*, 1605–1614. [[CrossRef](#)]
41. Pal, R. Modeling the viscosity of concentrated nanoemulsions and nanosuspensions. *Fluids* **2016**, *1*, 11. [[CrossRef](#)]
42. Pal, R. Modeling and scaling of the viscosity of suspensions of asphaltene nanoaggregates. *Energies* **2007**, *10*, 767. [[CrossRef](#)]
43. Ogunlaja, S.B.; Pal, R.; Sarikhani, K. Effects of starch nanoparticles on phase inversion of Pickering emulsions. *Can. J. Chem. Eng.* **2017**. [[CrossRef](#)]



© 2017 by the author. Licensee MDPI, Basel, Switzerland. This article is an open access article distributed under the terms and conditions of the Creative Commons Attribution (CC BY) license (<http://creativecommons.org/licenses/by/4.0/>).